



# Impact of traverse speed during joining of CDA101 plates using FSW process

B. Yokesh Kumar<sup>a</sup> and P. Sevel<sup>b,\*</sup>

a. *Department of Mechanical Engineering, Chennai Institute of Technology, Kundrathur – 600 069, Tamil Nadu, India.*

b. *Department of Mechanical Engineering, S.A. Engineering College, Chennai – 600 077, Tamil Nadu, India.*

Received 28 April 2021; received in revised form 3 September 2021; accepted 7 March 2022

## KEYWORDS

Traverse speed of tool;  
 CDA 101 Cu alloy;  
 Zone of stir;  
 Friction stir welding;  
 Tensile strength;  
 Micro-structural characteristics.

**Abstract.** This study conducts an experimental investigation to explore the impact of the traverse speed of a tool on the tensile strength and micro-structural peculiarities of joints attained during friction stir welding of Cu alloy namely CDA 101 flat plates. In this process, other parameters including spinning speed of tool (1100 rpm) and downward force (6 kN) were kept constant. A tool with a cylindrical tapered pin geometry was made to traverse at varying speeds, from 20 mm/min to 45 mm/min. It was observed that the CDA 101 joints fabricated at 20 mm/min were entirely free of flaws, while the joints fabricated at other traverse speeds of the tool were featured several weld flaws. Grains in the center of the stir zone of the joints obtained at 20 mm/min were uniformly distributed and homogeneous due to the significant volume of frictional heat and sufficient stirring force. The highest tensile strength of 200.65 MPa (nearly 85.38% of base metal) was exhibited by the joint attained at 20 mm/min.

© 2022 Sharif University of Technology. All rights reserved.

## 1. Introduction

Copper alloys have many use cases in different industrial sectors including marine systems, construction, and transportation for encapsulating material wastes, especially nuclear wastes, etc. This usage has become possible due to Copper alloys' superior thermal and electrical conductivities, unique combination of ductility and strength, exemplary resistance to corrosion, etc. [1–5].

Despite the everlasting demand for these alloys (Cu) in different industrial sectors, their usage has been limited due to the difficulty in welding them [6–

9]. Fusion-based joining techniques are not suitable for copper, given that the existence of pernicious and eruptive constituents such as zinc (present in the alloys of Cu) and other oxides (adherent in nature) deteriorates the welding quality [10–13]. In addition, peculiar features of Cu alloys including larger thermal diffusivity, elevated oxidation rate, etc. hinder successful welding of Cu alloys through fusion-based joining techniques [14,15].

Comparatively, unique and advanced solid conditions of welding methodology namely Friction Stir Welding (FSW), in which a non-esculent welding tool accomplishes both heat (due to friction) and mechanical deformation concurrently, appear to be suitable for joining Cu alloys [16–18]. Reasons for preferring the process of FSW for joining Cu are that the significant amount of heat input required for joining Cu alloys can be easily provided through the FSW process. In addition, this solid-state category of welding (i.e., FSW)

\*. *Corresponding author. Tel.: +91 94450 48418  
 E-mail address: yokeshkumarb@cit Chennai.net (B. Yokesh Kumar); drsevel@saec.ac.in (P. Sevel)*

makes it possible to attain superior high-strength joints free from cracks, porosity, and reduced levels of residual stresses [19–22].

The process of FSW is proved to be an effective joining method for almost all aluminum alloys (which could not be welded using conventional joining techniques) ranging from 7XXX alloy series to 2XXX series and several alloys of magnesium [23–31]. For example, FSW of 7-series Al alloy namely 7075-T6 Al alloy was carried out by Wen et al. [25]. In the course of this experimental attempt, they investigated the micro-structural and nano-mechanical characteristics of the fabricated 7075-T6 Al alloy joints utilizing the technique namely nano-indentation. Then, a correlation was framed between the micro-hardness and nano-hardness. Analysis of their experimental observations revealed that application of the FSW process led to the appreciable refinement of the grains, and the nano-hardness of each and every zone of the friction stir welded joint exhibited indentation size impact. Moreover, the nano-mechanical demeanor was proven to be impacted by precipitation in the interior of the grains. Likewise, Patel et al. [27] performed experimentation to attain very fine grains in Mg alloys with 6.35 mm thickness using copper and steel as backing plates by employing stationary shoulder-based friction stir technique. Uniform fine grains were obtained from the application of steel-type backing plates in the bottom, middle, and top regions of the stir zone, and they were 4.12, 4.75, and 4.98  $\mu\text{m}$  in size, respectively. Concurrently, copper-type backing plates produced very fine grains (0.96  $\mu\text{m}$  in size) in the lower region and fine grains (4.1  $\mu\text{m}$  in size) in the upper portion of the stir zone. The attainment of very fine grains contributed to a reasonable improvement in the hardness of the parent metal by nearly 80% and its tensile strength by nearly 24%.

Apart from joining similar alloys of Al, FSW was proved to be very much effective in welding dissimilar alloys of Al together. For instance, the experimental work of Shunmugasundaram et al. [29] investigated the optimization of parameters in a detailed manner during joining of dissimilar Al alloys, namely AA6063 and AA5052, through the FSW process. A major reason for conducting the joining of these dissimilar Al alloys is AA6063, which is of superior strength, whereas AA5052 is non-heat-treatable in nature and possesses desirable weldability; thereby, the fabricated joint possesses extra-ordinary properties. In this work, the FSW process parameters were optimized employing Taguchi-based L9 orthogonal array. The considered parameters included the speed of tool spinning, rate of traversing, and the angle of tool tilt and the optimization of these parameters aimed at the maximization of the strength (tensile) of the dissimilar joint. A close and detailed observation of the experimental recordings proved the

dominant role of the spinning speed of the tool in impacting the strength (tensile) of the fabricated joint when compared with other parameters, namely the rate of traversing and the angle of tool tilt.

Although the process of FSW was successfully employed for joining a wide variety of similar and dissimilar alloys of aluminum, only very few researchers [32–35] made investigational attempts to join Cu alloys employing the FSW process. For example, Nagabharam et al. [32] attempted to understand the impact of some FSW parameters, namely the geometry of tool pin, speed of traversing, and speed of spinning. In this experimental effort, tools with 2 distinctive geometries of pin (namely straight square and straight cylindrical) were employed at 2 distinctive traversing and spinning speeds. Validation of the experimental efforts revealed that Cu weldment fabricated at a tool spinning speed of 910 rpm and a traversing speed of 30 mm/min in the tool possessing square pin geometry exhibited desirable tensile strength, compared with that of other Cu joints.

Hwang et al. [34] investigated the thermal characteristics of the friction stir welded C11000 (pure copper) joints employing thermocouples (K-type) at distinctive locations on the surface of the plates to be welded and these thermocouples were employed to record the peak temperatures developed during the process of joining. The peak temperatures of the desirable quality joints were found to be in the range of 460°C to 530°C. Careful observations of the recorded data also demonstrated that the surfaces of the plates kept on the side of advancement experienced higher temperatures, compared with the plate surfaces on the side of retraction. The percentage of elongation exhibited by flawless joints was nearly 3 times larger than that of the parent metal, namely C11000.

Despite the limited scope of research on the impacts of parameters during the FSW of pure copper, no investigational works were accomplished to evaluate the impact of the speed of traverse during FSW of copper alloys. Significance of the traverse speed (i.e., feed rate), its impact on the evolution of micro-structural characteristics and joint quality, and inadequacy of research conclusions available with respect to FSW of copper alloys have motivated authors to perform this research investigation.

## 2. Procedure for experimentation

Copper alloy namely CDA 101 is the intended material for this experimentation. Flat plates (thickness of 6 mm, length of 150 mm, and width of 50 mm) of this CDA 101 alloy were butt joined using the FSW process. The composition of this material of experimental research is described in Table 1.

The tensile strength of experimented metal was 235 MPa along with yield strength of 193 MPa and

**Table 1.** Chemical configuration of CDA101.

Material	Pb	Si	Cr	Ni	P	S	Fe	Zn	Cu	less than < 0.001
CDA 101	< 0.005	< 0.005	< 0.01	< 0.005	< 0.005	< 0.002	< 0.015	0.0139	Balance	Mg, Sn, Al, Mn

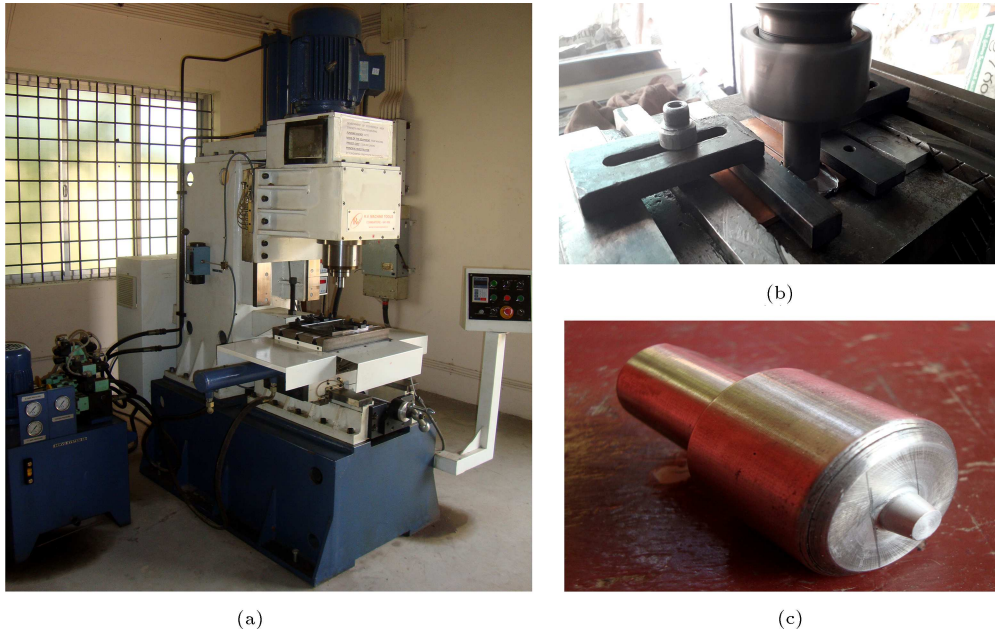


**Figure 1.** Photographs of (a) idiosyncratically developed, pseudo-automatic category friction stir welding machine employed in this work, (b) flat plates of base metal (CDA 101 alloy) being butt welded at right angles to the direction of rolling using FSW process, and (c) M42 grade HSS tool with cylindrically tapered profiled pin.

elongation of 18%. Flat plates of this base metal (CDA 101 alloy) were butt welded at right angles to the rolling direction, as seen in Figure 1(b), by employing an idiosyncratically developed, pseudo-automatic category friction stir welding machine, which can travel at three distinctive axes, i.e., 400 mm vertically, 510 mm longitudinally, and 400 mm horizontally. In addition, they were fitted with an 810 mm × 400 mm size work table. The photograph of this machine is shown in Figure 1(a). Moreover, the employed FSW machine encompasses an exclusive fabricated work holding platform so as to hold work pieces possessing the maximum width of 75 mm and the maximum length of 250 mm.

The employed tool possessed a 20 mm diameter shoulder for a length of 40 mm, followed by a 30 mm broad main shoulder for a 35 mm length possessing a cylindrically tapered pin profile for a length of 5.85 mm. The photograph of this tool is displayed in Figure 1(c). The tool used for carrying out the FSW in this experimental work was made out of M42 grade high-speed steel. The preminent reason for employing M42 grade HSS to fabricate tool in this work is that this grade of HSS additionally contains 8% of cobalt (when compared to other grades of HSS) and incorporation of this cobalt significantly increases the resistance of

heat of this alloy, leading to extraordinary red hardness properties as well as reduced welding and machining periods [36,37].

Another unique feature of this tool fabricated using M42 grade HSS is that it can last longer than M35, M2 grades of HSS [38,39]. The entire set of experimental investigations was carried out by employing a constant downward force of 6 kN and the tool was made to spin at a consistent speed of 1100 rpm and the tool was made to traverse at 6 distinctive rates including 20, 25, 30, 35, 40, and 45 mm/min.

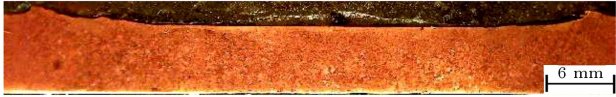





### 3. Experimental inferences and deliberations

#### 3.1. Characterization of macrostructures

Table 2 presents detailed macro-structural images of the friction stir welded CDA 101 flat plates obtained at 6 distinctive traverse speeds of the tool.

From this table, it can be visualized that the macrostructure of the CDA 101 flat plate joints fabricated at lower traverse speeds of the tool (i.e., at 20 mm/min) is free from flaws. Concurrently, with an upswing in the traverse speed of the tool (i.e., from 25 mm/min to 45 mm/min) and other adopted parameters remaining constant (namely 1100 rpm and 6 kN), the flaws and irregularities seem to get in-

**Table 2.** Macrostructure of the friction stir welded flat plates of CDA 101 at 6 distinctive traverse speeds of the tool.

Weldment no	Traverse speed of tool	Macrostructure of the friction stir welded plates of CDA 101
1	20 mm/min	
2	25 mm/min	
3	30 mm/min	
4	35 mm/min	
5	40 mm/min	
6	45 mm/min	

tensified. For example, the joint obtained during 25 mm/min is present with a weld flaw namely galling of surface, followed by tunneling flaws in CDA 101 joints fabricated at 30 and 35 mm/min. Likewise, the joints attained at 40 and 45 mm/min traverse speeds possess porosities.

### 3.2. Characterization of macrostructures

In order to gain a better understanding of the impact of the traverse speed of the employed tool during the welding of flat plates of CDA 101 by the FSW process, careful examinations of the respective joints microstructure are inevitable. The photographic images of the microstructures of the metal and CDA 101 friction stir welded joints fabricated at 6 distinctive traverse speeds of the tool are illustrated in Figure 2(a)–(g).

It can be seen in Figure 2(a) that the microstructure of the metal, i.e., CDA 101, possesses enormous sized grains with sporadic boundaries. The matrix of the metal exhibits the occupancy of coupled areas together with lines of assimilation. Careful observation of the microstructures of the friction stir welded CDA 101 joints, as in Figure 2(b)–(g), reveals that the process of friction stir welding has impacted the microstructural characteristics of this CDA 101 alloy and exceedingly refined the arrangement, distribution of the grains, and their size, especially in the region of the stir of the fabricated joints.

At the same time, it can be observed that there

exists a legitimate volume of difference in the size of the refined grains present in the region of the stir of all the CDA 101 joints fabricated at 20 mm/min to 45 mm/min, compared with that of their parent metal. This was principally due to the employment of the FSW process for joining the flat plates of CDA 101 alloy. Through the FSW process, the significant volume of the generated frictional heat has facilitated grain refinement, recrystallization, and distribution in a unique and compatible manner, as proven by Patel et al. [40].

At the same time, there exists a difference in the size of the grains due to the employment of 6 distinctive traverse speeds of the tool. For example, the grains found in the region of the stir of the joint fabricated at the tool traverse speeds of 30 mm/min (Figure 2(d)) and 35 mm/min (Figure 2(e)) were found to be smaller in size when compared with that of the grains present in the joints fabricated at 40 mm/min (Figure 2(f)) and 45 mm/min (Figure 2(g)).

Likewise, the grains present in the region of the stir of the joint fabricated at the tool traverse speeds of 20 mm/min (Figure 2(b)) and 25 mm/min (Figure 2(c)) are smaller in size compared with the grains present in the joints fabricated at 30 mm/min (Figure 2(d)) and 35 mm/min (Figure 2(e)). Thus, it can be understood that the joints fabricated at lower traverse speeds of the tool are found to possess fine sized, completely refined smaller sized uniaxial grains when compared with the joints fabricated at greater speeds of the tool traverse [41,42]. In other words, the

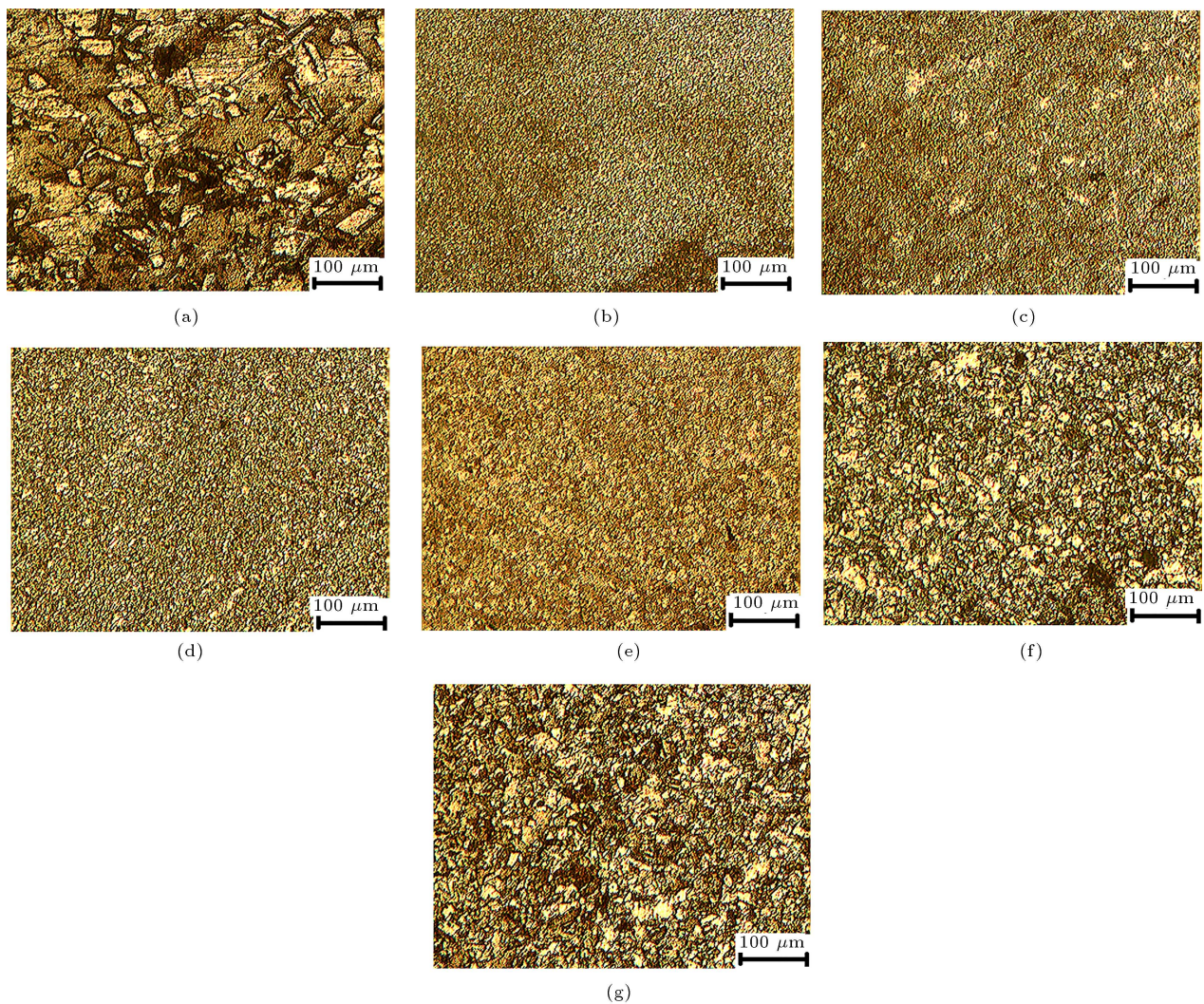


**Figure 2.** (a) Microstructure of the metal of investigation, i.e., CDA 101 alloy. Microstructure of the centre of the region of stir of CDA 101 joints attained at (b) 20 mm/min, (c) 25 mm/min, (d) 30 mm/min, (e) 35 mm/min, (f) 40 mm/min, and (g) 45 mm/min.

size of the grains seems to increase with an increase in the traverse speed of the tool.

This increase in the size of the grains parallel to an increase in the tool traverse speed occurs given that, as mentioned by Patel et al. [43], the high traverse speed of the tool would eventually lead to a reduction in deformation of friction stir welded joints [44]. A generally proven principle of recrystallization, as mentioned by Wang et al. [45], states that the reduced deformation degree following the employment of FSW for joining will increase the size of the recrystallized grains. This escalation in the size of the grains is usually associated with different weld deformities including surface galling, tunneling flaws, porosities, etc. [46,47]. As can be deduced from Table 2, the joints fabricated at higher tool traverse speeds were found to possess the above-mentioned defects, while those fabricated at a lower tool traverse speed (i.e., 20 mm/min) were completely free from defects.

### 3.3. Scrutiny of Scanning Electron Microscope (SEM) images

To have a better understanding of the evolution of microstructures in the friction stir welded CDA 101 flat plates, it is required to make a comparison among the Scanning Electron Microscope (SEM) images of different zones of the joints fabricated at lower and higher traverse speeds of the tool, 20 mm/min and 45 mm/min. Figure 3(a) depicts the SEM image of the metal under investigation, CDA 101 flat plate as the alloy of copper. This image reveals the presence of large-sized grains with sporadic boundaries.

Matrix of Cu metal also exhibits the occupancy of the coupled areas together with lines of assimilation. SEM images of the zones influenced by frictional heat (HAZ) of the joints fabricated at 20 mm/min and 45 mm/min are depicted in Figure 3(b) and (c), respectively. Based on the comparison of these two figures, it is clear that the grains of both joints in

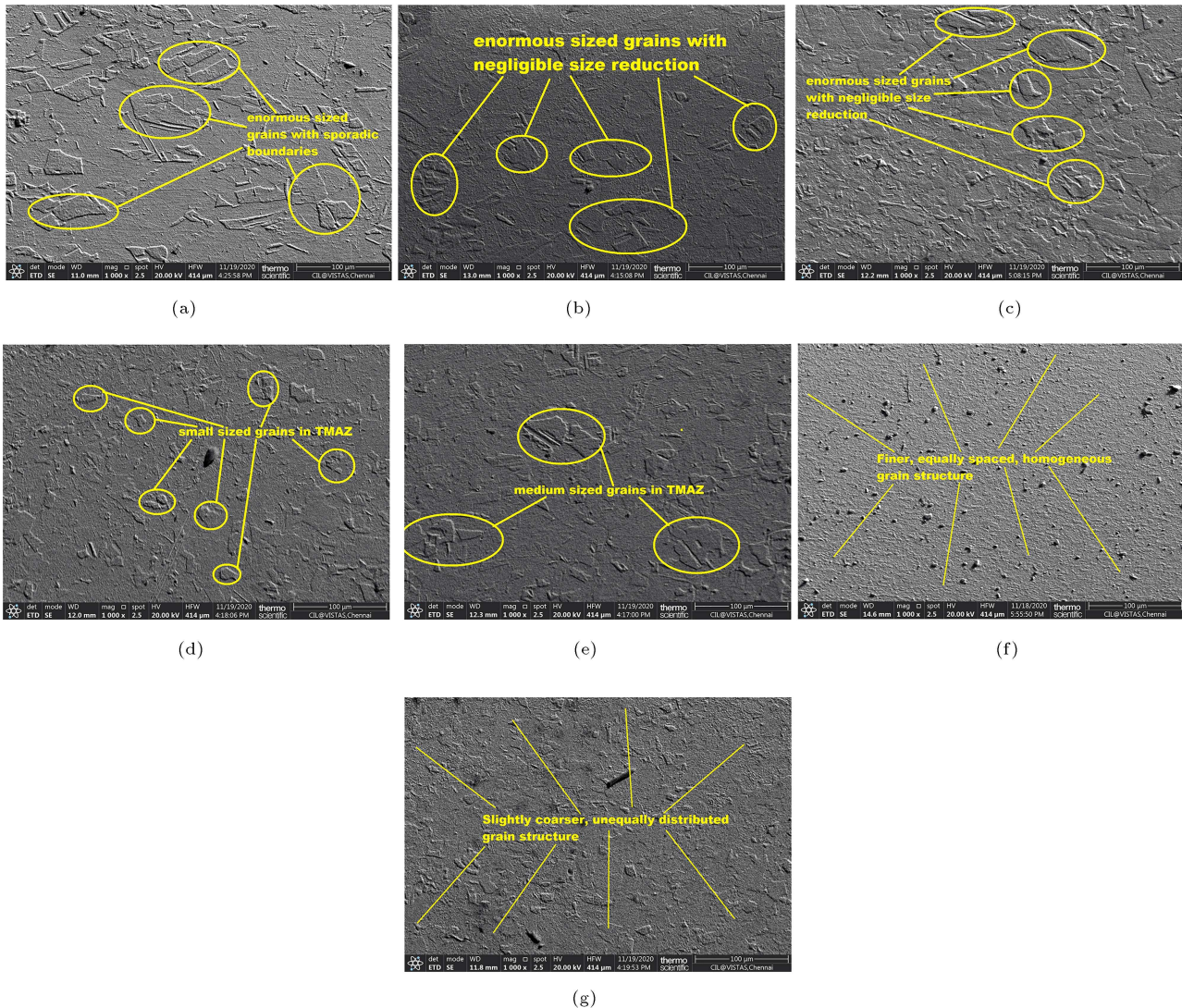


**Figure 3.** SEM image of (a) metal of investigation i.e., CDA 101. HAZ of the CDA 101 joint fabricated at (b) 20 mm/min and (c) 45 mm/min. TMAZ at (d) 20 mm/min and (e) 45 mm/min. Zone of stir at (f) 20 mm/min and (g) 45 mm/min.

the zone being influenced by heat have grown to some observable extent. At the same time, in both of the joints fabricated at 20 and 45 mm/min, we cannot observe any drastic change in the size of the grains when compared with their parent metal, demonstrating that the change in the traverse speeds of the tool has only a minor impact on the size of the grains in the HAZ.

Figure 3(d) and (e) portrays the SEM images of Thermo-Mechanically Affected Zone (TMAZ) by the joints fabricated at 20 mm/min and 45 mm/min. The size of the grains in the TMAZ of the joint fabricated at 20 mm/min seems to be smaller than that of the grains in the TMAZ of joints at 45 mm/min. It is understood that grains in the TMAZ of the joint fabricated at reduced traverse speeds of the tool have experienced sufficient frictional heat and a significant amount of stirring by using the shoulder of the tool for a

longer time period compared with the joint attained at 45 mm/min, which eventually played an inevitable role in reducing the size of the grains in the TMAZ [48,49].

Apart from this, it can be observed that in both of the Cu alloy joints (i.e., CDA 101 flat plate joints), the zone that is affected thermo mechanically is not as apparent as observed in the case of friction stir welded joints of aluminium or magnesium alloys [50]. This is because no stirred or lengthened grains contiguous to the zone of stir can be noticed. The SEM images of the zone of stir of the CDA 101 flat plate joints fabricated at 20 mm/min and 45 mm/min are portrayed in Figure 3(f) and (g), respectively. By correlating all these SEM images, we can see that the size of the grains in the TMAZ is tinier than that in the HAZ, but larger than those in the stir zone. The size of the grains in the stir zone in the joint attained at 20 mm/min is quite smaller than that of grains obtained at 45 mm/min.

Moreover, the grains at the center of the zone of stir of the joints obtained at the tool traverse speed of 20 mm/min are quite finer, uniaxially distributed, equally spaced, and homogeneous due to the significant volume of heat and much stirring exerted by the shoulder and pin of the tool for a sufficient period of time [51].

Even though the size of the grains of the joint attained at 45 mm/min is smaller than that in its base metal, it is noticeable that they are not finer and equally distributed when compared with the grains attained at 20 mm/min. This is mainly because the employment of higher tool traverse speeds (i.e., 45 mm/min) has subjected these grains to experience frictional heat and stirring action for a shorter period of time and this, in turn, led to these grain size variations and their distributions. These variations in grain size and their distributions eventually led to the welding defect like porosity in the joints fabricated at 45 mm/min. These findings prove that the traverse speed of the tool has an undeniable role in dominating the micro-structural features of attained joints of Cu alloy, namely CDA 101.

### 3.4. Determination of the mechanical strength

Figure 4 shows a graphical comparison of the tensile strength of the CDA 101 alloy weldments attained at varying traverse speeds of the tool. It can be observed that the tensile strength falls following an upswing in the tool traverse speed. Tensile strength of the joint attained at 20 mm/min seems to have the highest value, i.e., 200.65 MPa (nearly 85.38% of the tensile strength of the metal of investigation) and the lowest strength of 147.56 MPa is exhibited by the joint fabricated at a traversing speed of 45 mm/min.

Figure 5 depicts the locations of fracture of the CDA 101 Cu alloy joints fabricated at distinctive traverse speeds of the tool. Based on the careful observation of the images of the fractured tensile specimen of CDA 101 Cu alloy joints, we can visualize that reasonable necking prevails around the region of fracture for CDA 101 Cu alloy joint attained at 20 mm/min. It is implied that the macro-plastic type of deformation has occurred in that joint during the tensile strength test, as mentioned by Sejani et al. [52]. At the same time, this type of necking cannot be observed in the case of other joints when being subjected to the tensile load test. Moreover, the joint fabricated at 20 mm/min has encountered its fracture on the Side of Retraction (SR) and all other joints have encountered their fracture towards their Side of Advancement (SA). To be more specific, regarding the exact position of the exact location of the fracture mechanism, it can be stated that fracturing of the joint (attained at 20 mm/min) occurs along the thermo mechanically affected (TMAZ) and heat influenced

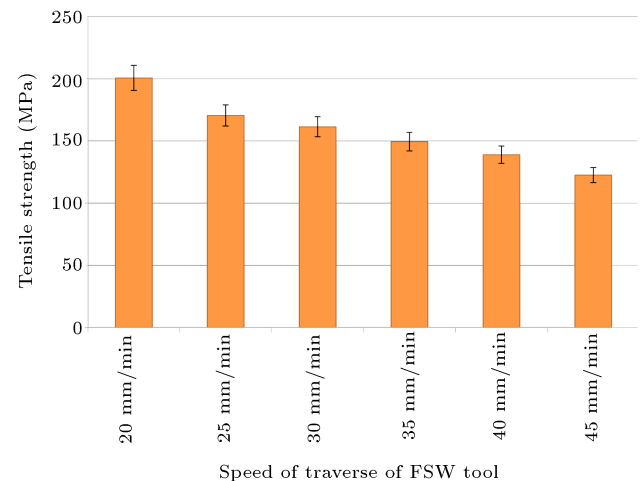


**Figure 4.** Graphical illustration of the tensile strength of the CDA 101 Cu alloy joints fabricated at distinctive traverse speeds of the FSW tool.



**Figure 5.** Photographs of the fractured tensile specimen of the CDA 101 Cu alloy joints with their exact location of fracture being highlighted.

(HAZ) regions. However, for all other joints, the fractures have occurred at the cavity of their defect [53].

### 3.5. Deliberations on SEM fractography

SEM tensile fractographic images of the joint attained at 20 mm/min are given in Figure 6(a) along with two highlighted portions namely 1, 2, and the enlarged SEM images of these two highlighted regions are displayed in Figure 6(b) and (c). From Figure 6(a), it can be found that the fractured sample of the CDA 101 Cu alloy joint possesses a fracture morphology, which is ductile in nature. This ductile type of fracture morphologies usually occurs due to amalgamation of micro voids present in its parent metal [40,45], which

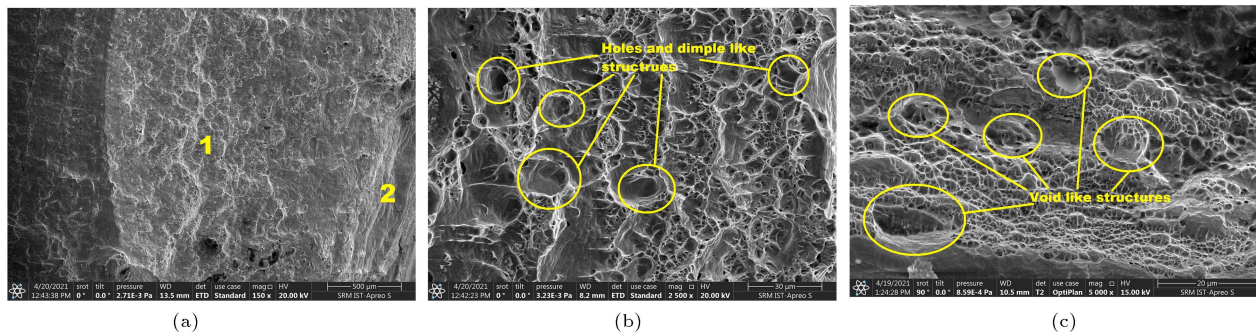


**Figure 6.** (a) SEM fractographic images of the tensile joints fabricated at 20 mm/min, (b) and (c) enlarged SEM images of the highlighted portions, namely 1 and 2.

is a positive indication that FSW has resulted in sound quality weldment. This fracture surface has been partitioned into two regions marked by 1 and 2; the magnified SEM images of these two regions are depicted in Figure 6(b) and (c).

Careful observations of the enlarged SEM images of these two marked regions reveal that the ridges and hole-like portions present in Figure 6(a) can be identified as dimples. These dimples are present in a river-like pattern along with the presence of very tiny void-like structures, indirectly confirming the higher ductility of the CDA 101, as a Cu alloy joint. Correlation between the presence of smaller sized grains and their uniform distribution in the zone of stir of the CDA 101 Cu alloy joint fabricated at 20 mm/min and the joint's tensile strength of 200.65 MPa (almost 85% of the parent metal) shows that the generation of these exquisite sized grains in the zone of stir resulting purely from the impact of the low traverse speed of the tool (20 mm/min) has made the joint entirely free from flaws, thus providing the required ideal amount of resistance to deformation during the tensile test, resulting in amalgamation of the micro voids of the parent metal and the ductile nature of the fracture morphology.

#### 4. Conclusions

In this experimental work, in the process of joining flat plates of Cu alloy namely CDA 101 using FSW, a detailed investigation was carried out to understand the impact of the traverse speed of the tool (with a cylindrically tapered pin geometry) on the micro-structural characteristics and mechanical properties of the obtained joints while keeping other parameters including speed of spinning of tool (1100 rpm) and downward force (6 kN) constant. The derived outcomes are mentioned below:

- CDA 101 Cu alloy joints fabricated at the tool traverse speed of 20 mm/min were observed to be entirely defect-free, while those fabricated at other

speeds (25 to 45 mm/min) were subject to several weld flaws including surface galling, porosities, tunneling flaws, etc.;

- A legitimate volume of difference in the size of the refined grains existed in the region of stir of all the CDA 101 joints fabricated at 20 mm/min to 45 mm/min, compared with that of their parent metal;
- CDA 101 Cu alloy joints fabricated at lower speeds (especially at 20 mm/min) possessed fine sized, completely refined smaller-sized uniaxial grains when compared with the joints fabricated at greater tool traverse speeds;
- Grains at the center of zone of stir of the joints obtained at 20 mm/min were finer in size, uniaxially distributed, equally spaced, and homogeneous, due to the significant volume of frictional heat as well as enormous stirring force and action exerted by shoulder and pin of the tool for sufficient period;
- Reasonable necking prevailed around the region of fracture for the CDA 101 Cu alloy joint attained at 20 mm/min, revealing that the macro-plastic type of deformation occurred in that joint during the tensile test;
- SEM tensile fractographic images of the joint attained at 20 mm/min reveals that the fracture morphology is ductile in nature and occurs due to the amalgamation of micro voids, positively indicating that employment of FSW for joining CDA 101 Cu alloys yielded sound quality weldment;
- Tensile strength was reduced with an increase in the tool traverse speed. Tensile strength of the joint attained at 20 mm/min exhibited the highest value, i.e., 200.65 MPa (nearly 85.38% of the tensile strength of the metal), while the lowest value of strength was exhibited by the joint fabricated at 45 mm/min traversing speed, namely 147.56 MPa.



## References

- Zhang, H., Jiao, K.X., Zhang, J.L., et al. “Experimental and numerical investigations of interface characteristics of copper/steel composite prepared by explosive welding”, *Materials & Design*, **154**, pp. 140–152 (2018).
- Sathiyaraj, S., Venkatesan, S., Ashokkumar, S., et al. “Wire electrical discharge machining (WEDM) analysis into MRR and SR on copper alloy”, *Materials Today Proceedings*, **33**(1), pp. 1079–1084 (2020).
- Dhanesh Babu, S.D., Sevel, P., Senthil Kumar, R., et al. “Development of thermo mechanical model for prediction of temperature diffusion in different FSW tool pin geometries during joining of AZ80A Mg alloys”, *Journal of Inorganic and Organometallic Polymers and Materials*, **66**(12), pp. 3196–3212 (2021).
- Silbernagel, C., Gargalis, L., Ashcroft, I., et al. “Electrical resistivity of pure copper processed by medium-powered laser powder bed fusion additive manufacturing for use in electromagnetic applications”, *Additive Manufacturing*, **29**, p. 100831 (2019).
- Dahaghin, Z., Zavvar Mousavi, H., Sajjadi, M., et al. “Determination and pre concentration of trace amounts of Cd(II), Cu(II), Ni(II), Zn(II), and Pb(II) ions by functionalized magnetic nanosorbent and optimization using a Box-Behnken design and detection of them by a flame atomic absorption spectrometer”, *Scientia Iranica*, **25**(6), pp. 3275–3287 (2018).
- Dhanesh Babu, S.D., Sevel, P., and Senthil Kumar, R. “Simulation of heat transfer and analysis of impact of tool pin geometry and tool speed during friction stir welding of AZ80A Mg alloy plates”, *Journal of Mechanical Science and Technology*, **34**(10), pp. 4239–4250 (2020).
- Wenhe Feng, Jiang Guo, Wenjin Yan, et al. “Deep channel fabrication on copper by multi-scan underwater laser machining”, *Optics & Laser Technology*, **111**, pp. 653–663 (2019).
- Liu, Y., Cai, S., Xu, F., et al. “Enhancing strength without compromising ductility in copper by combining extrusion machining and heat treatment”, *Journal of Materials Processing Technology*, **267**, pp. 52–60 (2019).
- Sathish, T., Sevel, P., Sudharsan, P., et al. “Investigation and optimization of laser welding process parameters for AA7068 aluminium alloy butt joint”, *Materials Today: Proceedings*, **37**, pp. 1672–1677 (2021).
- Ganachari, V.S., Chate, U.N., Waghmode, L.Y., et al. “A comparative performance study of dry and near dry EDM processes in machining of spring steel material”, *Materials Today Proceedings*, **18**(7), pp. 5247–5257 (2019).
- Wang, H., Wang, Y., Chi, G., et al. “Simulation study on surface drag reduction performance of beryllium copper alloy by EDM”, *Procedia CIRP*, **95**, pp. 244–249 (2020).
- Stephan Thangaiah, I.S., Sevel, P., Satheesh, C., et al. “Experimental study on the role of tool geometry in determining the strength & soundness of wrought AZ80a Mg alloy joints during FSW process”, *FME Transactions*, **46**(4), pp. 612–622 (2018).
- Azizi, A., Bayati, B., and Karamoozian, M. “A comprehensive study of the leaching behavior and dissolution kinetics of copper oxide ore in sulfuric acid lixiviant”, *Scientia Iranica*, **25**(3), pp. 1412–1422 (2018).
- Uhlmann, E., Kuche, Y., Polte, J., et al. “Influence of cutting edge micro-geometry in micro-milling of copper alloys with reduced lead content”, *Procedia CIRP*, **77**, pp. 662–665 (2018).
- Bagherzadeh, M., Mahmoudi, H., Amini, M., et al. “SBA-15-supported copper (II) complex: An efficient heterogeneous catalyst for azide-alkyne cycloaddition in water”, *Scientia Iranica*, **25**(3), pp. 1335–1343 (2018).
- Büttner, H., Vieira, G., Hajri, M., et al. “A comparison between micro milling pure copper and tungsten reinforced copper for electrodes in EDM applications”, *Precision Engineering*, **60**, pp. 326–339 (2019).
- Satheesh, C., Sevel, P., and Senthil Kumar, R. “Experimental identification of optimized process parameters for FSW of AZ91C Mg alloy using quadratic regression models”, *Strojniski Vestnik/Journal of Mechanical Engineering*, **66**(12), pp. 736–751 (2020).
- Boitsov, A.G., Pleshakov, A.S., Siluyanova, M.V., et al. “Friction stir welding of M1 copper alloy in the production of power equipment”, *Russian Engineering Research*, **40**(3), pp. 249–252 (2020).
- Saravanan, C., Saravanan, K., Sathish Kumar, G., et al. “Investigation and evaluation of mechanical behaviour of Al-TiC alloy”, *Materials Today: Proceedings*, **37**, pp. 1203–1207 (2021).
- Karrar, G., Galloway, A., Toumpis, A., et al. “Microstructural characterisation and mechanical properties of dissimilar AA5083-copper joints produced by friction stir welding”, *Journal of Materials Research and Technology*, **9**(5), pp. 11968–11979 (2020).
- Boitsov, A.G., Siluyanova, M.V., and Kuritsyna, V.V. “Electric-discharge milling of small airplane-engine components”, *Russian Engineering Research*, **38**(7) pp. 552–556 (2018).
- Kurtulmus, M. and Kiraz, A. “Artificial neural network modelling for polyethylene FSSW parameters”, *Scientia Iranica*, **25**(3), pp. 1266–1271 (2018).
- Langari, J. and Kolahan, F. “The effect of friction stir welding parameters on the microstructure, defects, and mechanical properties of AA7075-T651 joints”, *Scientia Iranica*, **26**(4), pp. 2418–2430 (2019).
- Li, W.Y., Niu, P.L., Yan, S.R., et al. “Improving microstructural and tensile properties of AZ31B magnesium alloy joints by stationary shoulder friction stir welding”, *Journal of Manufacturing Processes*, **37**, pp. 159–167 (2019).

25. Wang, W., Yuan, S., Qiao, K., et al. “Microstructure and nanomechanical behavior of friction stir welded joint of 7055 aluminum alloy”, *Journal of Manufacturing Processes*, **61**, pp. 311–321 (2021).
26. Zhang, H.J., Sun, S.L., Liu, H.J., et al. “Characteristic and mechanism of nugget performance evolution with rotation speed for high-rotation-speed friction stir welded 6061 aluminum alloy”, *Journal of Manufacturing Processes*, **60**, pp. 544–552 (2020).
27. Patel, V., Li, W., Liu, X., et al. “Tailoring grain refinement through thickness in magnesium alloy via stationary shoulder friction stir processing and copper backing plate”, *Materials Science and Engineering: A*, **784**, p. 139322 (2020).
28. Sevel, P. and Satheesh, C. “Role of tool rotational speed in influencing microstructural evolution, residual-stress formation and tensile properties of friction-stir welded AZ80A Mg alloy”, *Materiali in Tehnologije*, **52**(5), pp. 607–614 (2018).
29. Shunmugasundaram, M., Praveen Kumar, A., Ponraj Sankar, L., et al. “Optimization of process parameters of friction stir welded dissimilar AA6063 and AA5052 aluminum alloys by Taguchi technique”, *Materials Today: Proceedings*, **27**(2), pp. 871–876 (2020).
30. Sevel, P., Dhanesh Babu, S.D., and Senthil Kumar, R. “Peak temperature correlation and temperature distribution during joining of AZ80A Mg alloy by FSW – A numerical and experimental investigation”, *Strojnikski vestnik - Journal of Mechanical Engineering*, **66**(6), pp. 395–407 (2020).
31. Sevel, P. and Jaiganesh, V. “Investigation on evolution of microstructures and characterization during FSW of AZ80A Mg alloy”, *Archives of Metallurgy and Materials*, **62**(3), pp. 1779–1785 (2017).
32. Nagabharam, P., Srikanth Rao, D., Manoj Kumar, J., et al. “Investigation of mechanical properties of friction stir welded pure copper plates”, *Materials Today: Proceedings*, **5**, pp. 1264–1270 (2018).
33. Xu, N., Feng, R.N., Guo, W.F., et al. “Effect of Zener-Hollomon parameter on microstructure and mechanical properties of copper subjected to friction stir welding”, *Acta Metallurgica Sinica (English Letters)*, **33**, pp. 319–326 (2020).
34. Hwang, Y.M., Fan, P.L., and Lin, C.H. “Experimental study on friction stir welding of copper metals”, *Journal of Materials Processing Technology*, **210**(12), pp. 1667–1672 (2010).
35. Jha, K., Kumar, S., Nachiket, K., et al. “Friction Stir Welding (FSW) of aged CuCrZr alloy plates”, *Metallurgical and Materials Transactions A*, **49**, pp. 223–234 (2018).
36. Ramkumar, S., Duraiselvam, M., and Sevel, P. “Acoustic emission based deep learning technique to predict adhesive bond strength of laser processed CFRP composites”, *FME Transactions*, **48**(3), pp. 611–619 (2020).
37. Chai, F., Yan, F., Wang, W., et al. “Microstructures and mechanical properties of AZ91 alloys prepared by multi-pass friction stir processing”, *Journal of Materials Research*, **33**, pp. 1789–1796 (2018).
38. Joshi, G.R. and Badheka, V.J. “Microstructures and properties of copper to stainless steel joints by hybrid FSW”, *Metallography, Microstructure, and Analysis*, **6**, pp. 470–480 (2017).
39. Sevel, P., Satheesh, C., and Senthil Kumar, R. “Generation of regression models and multi-response optimization of friction stir welding technique parameters during the fabrication of AZ80A Mg alloy joints”, *Transactions of the Canadian Society for Mechanical Engineering*, **44**(2), pp. 311–324 (2020).
40. Patel, V., Li, W., Vairis, A., et al. “Recent development in friction stir processing as a solid-state grain refinement technique: microstructural evolution and property enhancement”, *Critical Reviews in Solid State and Materials Sciences*, **44**(5), pp. 378–426 (2019).
41. Patel, P., Rana, H., Badheka, V., et al. “Effect of active heating and cooling on microstructure and mechanical properties of friction stir-welded dissimilar aluminium alloy and titanium butt joints”, *Welding in the World*, **64**, pp. 365–378 (2020).
42. Lin, J., Zhang, D.T., Zhang, W., et al. “Microstructure and mechanical properties of ZK60 magnesium alloy prepared by multi-pass friction stir processing”, *Materials Science Forum*, **898**, pp. 278–283 (2017).
43. Patel, V., Li, W., Liu, X., et al. “Through-thickness microstructure and mechanical properties in stationary shoulder friction stir processed AA7075”, *Materials Science and Technology*, **35**(14), pp. 1762–1769 (2019).
44. Esmaily, M., Svensson, J.E., Fajardo, S., et al. “Fundamentals and advances in magnesium alloy corrosion”, *Progress in Materials Science*, **89**, pp. 92–193 (2017).
45. Wang, Y., Fu, R., Jing, L., et al. “Grain refinement and nanostructure formation in pure copper during cryogenic friction stir processing”, *Materials Science and Engineering: A*, **703**, pp. 470–476 (2017).
46. Sun, T., Roy, M.J., Strong D., et al. “Weld zone and residual stress development in AA7050 stationary shoulder friction stir T-joint weld”, *Journal of Materials Processing Technology*, **263**, pp. 256–265 (2019).
47. Qin, D.Q., Fu, L., and Shen, Z.K. “Visualisation and numerical simulation of material flow behaviour during high-speed FSW process of 2024 aluminium alloy thin plate”, *International Journal of Advanced Manufacturing Technology*, **102**, pp. 1901–1912 (2019).
48. Jaiganesh, V. and Sevel, P. “Effect of process parameters in the microstructural characteristics and mechanical properties of AZ80A Mg alloy during friction stir welding”, *Transactions of the Indian Institute of Metals*, **68**(S1), pp. 99–104 (2015).
49. Shahnam, A., Karimzadeh, F., Golozar, M.A., et al. “Microstructure evolution of ultra-fine-grained AZ31 B magnesium alloy produced by submerged friction

stir processing”, *Journal of Materials Engineering and Performance*, **28**, pp. 4593–4601 (2019)

50. Sevel, P., Satheesh, C., and Jaiganesh, V. “Influence of tool rotational speed on microstructural characteristics of dissimilar Mg alloys during friction stir welding”, *Transactions of the Canadian Society for Mechanical Engineering*, **43**(1), pp. 132-141 (2019).
51. Gao, J., Zhang, S., Jin, H., et al. “Fabrication of Al7075/PI composites base on FSW technology”, *International Journal of Advanced Manufacturing Technology*, **104**, pp. 4377–4386 (2019).
52. Sejani, D., Li, W., and Patel, V. “Stationary shoulder friction stir welding–low heat input joining technique: a review in comparison with conventional FSW and bobbin tool FSW”, *Critical Reviews in Solid State and Materials Sciences*, **2**, pp. 1–50 (2021).
53. Anil Kumar, K.S., Murigendrappa, S.M., and Kumar, H. “Experimental investigation on effects of varying volume fractions of SiC nanoparticle reinforcement on microstructure and mechanical properties in friction-stir-welded dissimilar joints of AA2024-T351 and AA7075-T651”, *Journal of Materials Research*, **34**, pp. 1229–1247 (2019).

## Biographies

**B. Yokesh Kumar** is currently pursuing his PhD degree in Mechanical Engineering, Anna University, Chennai, India. He had successfully completed his MS degree with 1st Class in Industrial Engineering from Anna University, Chennai, India in 2014. He

has a total 7.5 years of teaching experience. He is currently serving as an Assistant Professor at the Department of Mechanical Engineering, Chennai Institute of Technology, Chennai, TamilNadu, India. He has published several research papers in the area of friction stir welding in renowned international journals indexed in Science Citation Index, Scopus, etc.

**P. Sevel** obtained his PhD in Mechanical Engineering from Anna University, Chennai in 2016 and successfully completed his MTech degree with 1st Class Distinction in Industrial Engineering from the National Institute of Technology (NIT) Trichy, India in 2005. He has a total of more than 15 years of teaching experience. He is currently working as a Professor, in Department of Mechanical Engineering College in S.A. Engineering College, Chennai. He has a total of 3 ongoing funded Projects worth Rs. 46,90,107 under various schemes of DST, TNSCST. He has 5 Indian PATENT GRANTS in his name. He is a Life Member of the Indian Society for Technical Education (ISTE) and a Corporate Member in The Institution of Engineers (IE), India. He has published more than 46 research papers in various SCI and Scopus indexed international journals. He is currently guiding a total of 9 research scholars pursuing their PhD at Center for Research, Anna University. He was awarded BEST RESEARCHER AWARD for his distinct contribution to the field of Materials Science during the 6th Annual Millennium Impact Award 2020.